Optimal Clustering of Energy-Harvesting Base Stations

Doris Benda*, Xiaoli Chu*, Sumei Sun†, Tony Q.S. Quek‡ and Alastair Buckley*
* University of Sheffield, United Kingdom
† Institute for Infocomm Research, A*STAR, Singapore
‡ Singapore University of Technology and Design, Singapore
E-mail: dcbenda1@sheffield.ac.uk, x.chu@sheffield.ac.uk, sunsm@i2r.a-star.edu.sg,
tonyquek@sutd.edu.sg, alastair.buckley@sheffield.ac.uk

Abstract*—Renewable energy can be used more efficiently in a cellular network if renewable-energy harvesters with anti-correlated energy generation profiles are deployed at neighboring base stations (BSs) and if the renewable energy can be shared among BSs via transmission lines. There are two different energy harvesters, which have anti-correlated energy generation profiles, available for deployment at the BSs in our system model. We develop a BS clustering optimization algorithm that can be run once during the cellular network planning to determine which out of the two types of energy harvesters should be deployed to every BS, i.e., BSs grouped into one cluster by the algorithm will be equipped with the same type of energy harvester. The optimization objective is to maximize the renewable power that can be shared in the cellular network. We take into account the topology of the cellular network, i.e., whether or not a transmission line exists between a pair of BSs, and the distance-dependent power loss in the transmission lines during the optimization. We investigate the performance of our proposed BS clustering optimization algorithm in comparison with randomly allocating the BSs into clusters, i.e., without considering the topology of the cellular network or the power losses in the transmission lines, for different numbers of BSs, for different transmission line existence probabilities, for different power loss coefficients per l meters of transmission line, and for different power surplus values. The normalized renewable power shared in the cellular network of our proposed BS clustering optimization algorithm in comparison with a random cluster allocation is on average around 40% higher.

***Index Terms*—Cellular network, energy generation diversification, energy harvesting, energy sharing**

I. Introduction

Energy generation diversification has been shown to improve the reliability of a renewable-powered cellular network. It is especially promising to combine energy generation harvesters which have anti-correlated energy generation profiles and to share the power by transmitting power from surplus BSs to deficit BSs via transmission lines [1]. For instance, 80% of power can be saved if power sharing is conducted between two base stations (BSs) with anti-correlated sinusoidal energy profiles [2]. Another example is to combine a wind energy harvester and a solar energy harvester. The anti-correlation between solar and wind energy generation profiles is justified on a daily timescale by the fact that high (low) pressure areas tend to be sunny (cloudy) with low (high) surface wind, and on a seasonal timescale by the fact that more solar (wind) energy can be harvested in summer (winter) than in winter (summer) for many locations [3].

To demonstrate the concept of anti-correlated energy harvesters, we use a southeast orientated photovoltaic (PV) cell (energy harvester type 0) and a southwest orientated PV cell (energy harvester type 1) in London in June as an example. A southeast (southwest) orientated PV cell has an orientation angle of $-45°$ ($45°$) with respect to the southern direction (cf. Fig. 1). While energy harvester type 0 has a high power generation during time step 1 (potential surplus), energy harvester type 1 suffers from a low power generation (potential deficit) during this time step (cf. Fig. 2). Vice versa in time step 2, while energy harvester type 0 has a low power generation (potential deficit), energy harvester type 1 has a high power generation (potential surplus) during this time step. To make efficient use of the renewable power, power should be shared from BSs equipped with energy harvester type 0 to BSs equipped with energy harvester type 1 in time step 1. Vice versa in time step 2, power should be shared from BSs equipped with energy harvester type 1 to BSs equipped with energy harvester type 0.

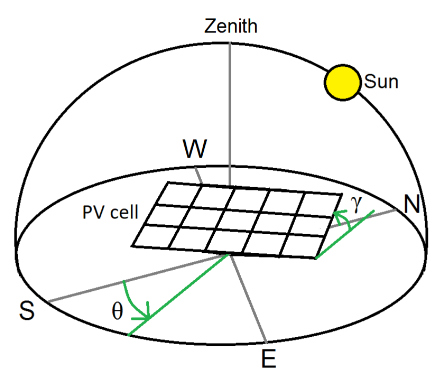

Fig. 1: Depiction of a PV cell installed with the orientation angle $\theta = -45°$ and with the inclination angle $\gamma = 38°$. We use the orientation angle and inclination angle definition from [4].

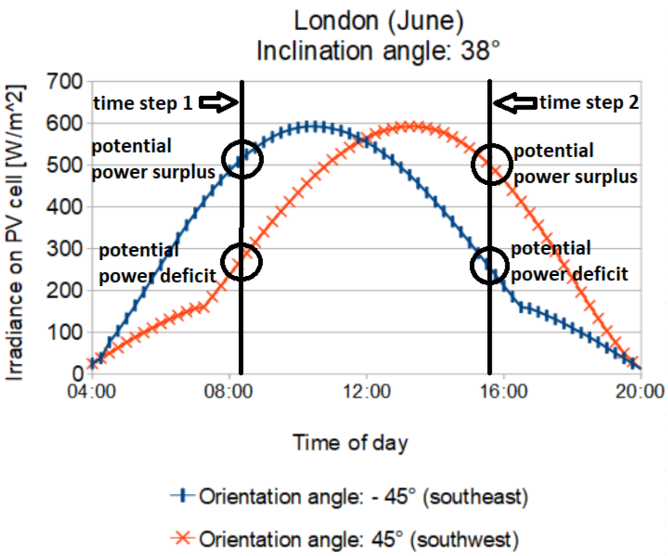

Fig. 2: A southeast orientated PV cell and a southwest orientated PV cell in London in June are used to demonstrate the concept of anti-correlated energy harvesters. Data source: [5]

II. System Model

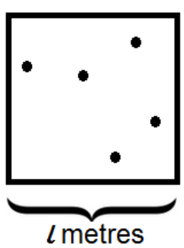

Fig. 3: Illustration of the considered cellular network with $N = 5$ BSs uniformly distributed in a square area of l^2 square meters.

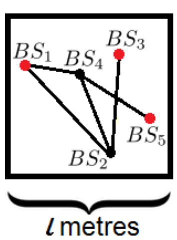

i	c_i	p_i^1	p_i^2
1	1	b_1	b_0
2	0	b_0	b_1
3	1	b_1	b_0
4	0	b_0	b_1
5	1	b_1	b_0

Fig. 4: The graph representation of the cellular network with example BS cluster allocation values c_i, surplus/deficit power values p_i^1 in time step 1 and surplus/deficit power values p_i^2 in time step 2 given for the BSs.

We consider $N \in \mathbb{N}$ uniformly distributed BSs in a square area of l^2 square meters (cf. Fig. 3), which are denoted as BS_i, $i \in \{1, ..., N\}$. The parameter $c_i \in \{0, 1\}$ denotes if the BS_i is equipped with the energy harvesting device type 0 or the energy harvesting device type 1, e.g., either with a solar cell or a wind turbine. A BS_i with energy harvesting device type 0, i.e., $c_i = 0$, belongs to cluster 0 and is depicted with a black node in Fig. 4. A BS_i with energy harvesting device type 1, i.e., $c_i = 1$, belongs to cluster 1 and is depicted with a red node in Fig. 4.

The BS clustering optimization algorithm will be run once during the construction of the cellular network to determine for every BS if it should belong to cluster 0 and hence be equipped with energy harvesting device type 0 or if it should belong to cluster 1 and hence be equipped with energy harvesting device type 1. After the energy harvesting devices are deployed at the BSs, a BS cannot change its cluster anymore.

The difference between the power generation and consumption of BS_i is denoted as the power surplus/deficit value $p_i^t[W]$ in watts for time step $t \in \{1, 2\}$. A surplus and deficit in power at BS_i is indicated by a positive and a negative value p_i^t, respectively. The power surplus/deficit value of BSs in the same cluster at a given time step are similar because they are equipped with the same energy harvesting device type, hence we assume that all BSs in the same cluster have the same power surplus/deficit value at a given time step.

The energy generation profile of BSs in cluster 0 is anti-correlated to the energy generation profile of BSs in cluster 1. In other words, BSs of cluster 0 and cluster 1 have a power surplus of $b_0 \in \mathbb{R}^+$ and power deficit of $b_1 \in \mathbb{R}^-$ in time step 1, respectively. Vice versa in time step 2, BSs of cluster 0 and cluster 1 have a power deficit of b_1 and power surplus of b_0, respectively. The power surplus/deficit values p_i^t are summarized as follows:

$$p_i^t = \begin{cases} b_0 & c_i = 0 \text{ and } t = 1 \\ b_1 & c_i = 1 \text{ and } t = 1 \\ b_1 & c_i = 0 \text{ and } t = 2 \\ b_0 & c_i = 1 \text{ and } t = 2. \end{cases} \quad (1)$$

We normalize the Euclidean distance $d\big((i,j)\big)$ between BS_i and BS_j with respect to l meters as follows:

$$d\big((i,j)\big) = \frac{||BS_i - BS_j||}{l}, \quad (2)$$

where $||BS_i - BS_j||[\mathrm{m}]$ in meters is the Euclidean distance between BS_i and BS_j and $l[m]$ in meters is the side length of the square in Fig. 4.

Power can be shared from a surplus BS_i in cluster 0 to a deficit BS_j in cluster 1 in time step 1 if BS_i and BS_j are connected by a transmission line. Vice versa in time step 2, power can be shared from a surplus BS_j in cluster 1 to a deficit BS_i in cluster 0 if BS_i and BS_j are connected by a transmission line. The power flow in the transmission line is subject to power loss due to resistive heating. The power loss $P_{\text{loss}}\big((i,j)\big)[\mathrm{W}]$ in watts in the transmission line from BS_i to BS_j can be calculated by Ohm's law and the formula for the transmission line resistance [6] as follows:

$$P_{\text{loss}}\big((i,j)\big) = I^2 \cdot \rho \cdot \frac{l \cdot d\big((i,j)\big)}{A_c} = I^2 \cdot C \cdot d\big((i,j)\big), \quad (3)$$

where $I[\mathrm{A}]$ in amperes is the electric current traveling through the transmission line, $\rho[\Omega\mathrm{m}]$ in ohm-meters is the resistivity of the transmission line, $l[\mathrm{m}]$ in meters is the side length of the square in Fig. 4, $d\big((i,j)\big)$ is defined in (2), $A_c[\mathrm{m}^2]$ in square meters is the cross-sectional area of the transmission line and $C[\Omega]$ in ohms is the power loss coefficient per l meters of transmission line, i.e., $C = \frac{\rho \cdot l}{A_c}$.

The topology of the cellular network is represented by a graph (cf. Fig. 4), where V is the set of vertices which denotes the BSs and E is the set of directed edges which denotes the transmission lines as follows:

$$
\begin{aligned}
V =& \{1,2,...,N\} \\
E =& \{(i,j),(j,i) | i \in V, j \in V, i \text{ and } j \text{ are} \\
& \text{connected by a transmission line}\},
\end{aligned} \tag{4}
$$

where (i,j) denotes the directed edge from BS_i to BS_j.

The power flow on the edge (i,j) is denoted as $f^t\big((i,j)\big)$ in time step $t \in \{1,2\}$.

We justify the following two assumptions in our system model.

- The power flow is equivalent to the second power of the electric current flow in the transmission line:
  The electric power P in the transmission line can be calculated as follows:
  $$P = V \cdot I, \tag{5}$$
  where V is the electric potential and I is the electric current. The power loss $P_{\text{loss}}\big((i,j)\big)$ in the transmission line is caused by the electric current and not the electric potential of the power as seen in (3). Nonetheless, it is outside of the scope of this paper to model the relationship between the power flow and the electric current flow in the transmission line. Hence, we assume for simplicity and in accordance with (5) that if the power increases/decreases in the transmission line, the electric current and the electric potential increase/decrease equally. In other words, a power flow in the transmission line of x watts is equivalent to a flow of $I = \sqrt{x}$ amperes and $V = \sqrt{x}$ voltages in our system model. Hence, the parameter $f^t\big((i,j)\big)[W/A^2]$ can be interpreted as the power flow on the edge (i,j) in watts or the second power of the current flow I^2 on the edge (i,j) in square amperes.
- $C \in \big[0, \frac{1}{\sqrt{2}}\big]$:
  The maximum normalized distance $d\big((i,j)\big)$ in a square is $\sqrt{2}$. If C were greater than $\frac{1}{\sqrt{2}}$, then $C \cdot d\big((i,j)\big)$ could be greater than 1. That would imply that more power is lost in the transmission line than was sent through the transmission line.

We normalize all power values with respect to $\max\{b_0, |b_1|\}$ as follows:

$$
\begin{aligned}
\hat{f}^t\big((i,j)\big) &= \frac{f^t\big((i,j)\big)}{\max\{b_0,|b_1|\}} \\
\hat{b}_0 &= \frac{b_0}{\max\{b_0,|b_1|\}} \\
\hat{b}_1 &= \frac{b_1}{\max\{b_0,|b_1|\}.}
\end{aligned} \tag{6}
$$

III. Mixed-Integer Linear Programming Problem

The objective is to find the optimal BS cluster allocation values c_n for all $BS_n, n \in V$, i.e., deploying either an energy harvesting device type 0 or an energy harvesting device type 1 at every BS, so that the renewable power in the cellular network can be used most efficiently. c_n, $\hat{f}^1\big((i,j)\big)$ and $\hat{f}^2\big((i,j)\big)$ are the parameters to be determined for all $n \in V$ and $(i,j) \in E$. Because the parameters c_n are integers whereas the power flow values $\hat{f}^t\big((i,j)\big)$ are real numbers, we need a mixed-integer linear programming solver for this problem.

The optimization objective is to maximize the total normalized renewable power M received at the deficit BSs during the two time steps as follows:

$$
\begin{aligned}
M = \max_{\mathbf{c},\hat{\mathbf{f}}^1,\hat{\mathbf{f}}^2} \Big\{ & \underbrace{\sum_{(i,j)\in E} \hat{f}^1\big((i,j)\big)\big(1 - C \cdot d\big((i,j)\big)\big)}_{\text{time step 1}} \\
& + \underbrace{\sum_{(i,j)\in E} \hat{f}^2\big((i,j)\big)\big(1 - C \cdot d\big((i,j)\big)\big)}_{\text{time step 2}} \Big\}
\end{aligned} \tag{7}
$$

subject to

Lower bounds and upper bounds for the parameters to be determined:

$$
\begin{aligned}
& 0 \le c_n \le 1, \quad c_n \in \mathbb{Z}, \quad \forall n \in V \\
& \left.0 \le \hat{f}^1\big((i,j)\big) \le 1 \quad \forall (i,j) \in E \right\} \text{time step 1} \\
& \left.0 \le \hat{f}^2\big((i,j)\big) \le 1 \quad \forall (i,j) \in E \right\} \text{time step 2}
\end{aligned} \tag{8}
$$

Power flow only on edges from surplus BSs to deficit BSs:

$$
\begin{aligned}
& \left.\begin{aligned} \hat{f}^1\big((i,j)\big) + c_i \le 1 \quad \forall (i,j) \in E \\ \hat{f}^1\big((i,j)\big) - c_j \le 0 \quad \forall (i,j) \in E \end{aligned}\right\} \text{time step 1} \\
& \left.\begin{aligned} \hat{f}^2\big((i,j)\big) + c_j \le 1 \quad \forall (i,j) \in E \\ \hat{f}^2\big((i,j)\big) - c_i \le 0 \quad \forall (i,j) \in E \end{aligned}\right\} \text{time step 2}
\end{aligned} \tag{9}
$$

Power flow out of the surplus BSs:

$$
\begin{aligned}
& \left.\sum_{\substack{(i,j)\in E \\ j\in V}} \hat{f}^1\big((i,j)\big) \le \hat{b}_0 \quad \forall i \in V \right\} \text{time step 1} \\
& \left.\sum_{\substack{(i,j)\in E \\ j\in V}} \hat{f}^2\big((i,j)\big) \le \hat{b}_0 \quad \forall i \in V \right\} \text{time step 2}
\end{aligned} \tag{10}
$$

Power flow into the deficit BSs:

$$
\begin{aligned}
& \underbrace{\sum_{\substack{(i,j)\in E \\ i\in V}} \hat{f}^1\big((i,j)\big)\big(1 - C \cdot d\big((i,j)\big)\big) \le |\hat{b}_1| \quad \forall j \in V}_{\text{time step 1}} \\
& \underbrace{\sum_{\substack{(i,j)\in E \\ i\in V}} \hat{f}^2\big((i,j)\big)\big(1 - C \cdot d\big((i,j)\big)\big) \le |\hat{b}_1| \quad \forall j \in V}_{\text{time step 2}}
\end{aligned} \tag{11}
$$

The optimization objective (7) adds the normalized power flows on all edges and subtracts the normalized power losses (cf. (3)) on all edges.

The inequalities (8) represent the lower bounds and the upper bounds for the parameters to be determined, i.e., for the parameters c_n, $\hat{f}^1\big((i,j)\big)$ and $\hat{f}^2\big((i,j)\big)$ for all $n \in V$ and $(i,j) \in E$. In addition, the inequalities (8) state that the parameters c_n are integers for all $n \in V$.

The inequalities (9) ensure that power only flows on edges from surplus BSs to deficit BSs. Power can only flow on an edge (i,j) in time step 1 if BS_i belongs to cluster 0, i.e., $c_i = 0$, and BS_j belongs to cluster 1, i.e., $c_j = 1$. $\hat{f}^1\big((i,j)\big)+c_i \leq 1$ implies that the power flow $\hat{f}^1\big((i,j)\big)$ is 0 if c_i is not 0 and $\hat{f}^1\big((i,j)\big)-c_j \leq 0$ implies that the power flow $\hat{f}^1\big((i,j)\big)$ is 0 if c_j is not 1 in time step 1. Vice versa in time step 2, power can only flow on an edge (i,j) if BS_i belongs to cluster 1, i.e., $c_i = 1$, and BS_j belongs to cluster 0, i.e., $c_j = 0$. $\hat{f}^2\big((i,j)\big) + c_j \leq 1$ implies that the power flow $\hat{f}^2\big((i,j)\big)$ is 0 if c_j is not 0 and $\hat{f}^2\big((i,j)\big) - c_i \leq 0$ implies that the power flow $\hat{f}^2\big((i,j)\big)$ is 0 if c_i is not 1 in time step 2.

The inequalities (10) ensure that the normalized power flow out of a surplus BS is not greater than $\hat{b}_0$. If $i \in V$ is a deficit BS in time step t then $\sum_{\substack{(i,j)\in E\\ j\in V}} \hat{f}^t\big((i,j)\big) \leq \hat{b}_0$ is already fulfilled because all power flows out of the deficit BS_i are 0 due to the inequalities (9).

The inequalities (11) ensure that the normalized power flow into a deficit BS is not greater than $|\hat{b}_1|$. The power received at the deficit BSs is subject to power losses in the transmission lines. If $j \in V$ is a surplus BS in time step t then $\sum_{\substack{(i,j)\in E\\ i\in V}} \hat{f}^t\big((i,j)\big)\big(1 - C \cdot d\big((i,j)\big)\big) \leq |\hat{b}_1|$ is already fulfilled because all power flows into the surplus BS_j are 0 due to the inequalities (9).

IV. Numerical Results

We use the intlinprog(f, intcon, A, b) function implemented in MATLAB to solve the mixed-integer linear programming problem (MILPP) defined in (7)-(11). Unless otherwise stated, we use the values from Table I for the parameters to evaluate the performance of our proposed MILPP.

TABLE I: Input parameters

Parameter	Value
$C \in [0, \frac{1}{\sqrt{2}}]$	0.6
$N \in \mathbb{N}$	8
$q \in [0,1]$	0.3
$b_0 \in \mathbb{R}^+$	1
$b_1 \in \mathbb{R}^-$	-1

We generate 1000 random graphs to determine the average normalized renewable power M received at the deficit BSs during the two time steps (cf. (7)). The random graphs are generated by placing the N BSs uniformly in the square and connecting any two BSs with a probability of $q \in [0,1]$ with a transmission line. We investigate the performance of our proposed MILPP in comparison with randomly allocating BSs into clusters, i.e., without considering the topology of the cellular network or the power losses in the transmission lines by setting the cluster allocation values c_i to 0 and 1 with a probability of 50% and 50%, respectively. In other words, $\mathbb{P}(c_i = 0) = \mathbb{P}(c_i = 1) = 0.5\ \forall i$ for the random cluster allocation.

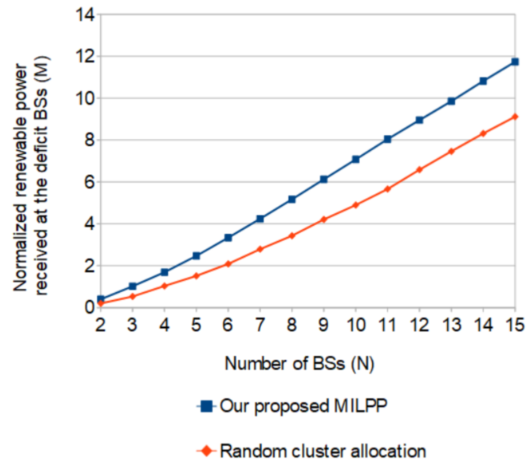

Fig. 5: Average normalized renewable power received at the deficit BSs (M) of our proposed MILPP and of random BS cluster allocation vs. number of BSs (N).

Fig. 5 shows the performance of our proposed MILPP and of random BS cluster allocation for different numbers of BSs (N). The performance gap between the two BS cluster allocations increases with the number of BSs. This is because a denser cellular network offers more opportunities for BS clustering optimization, and hence the superiority of the MILPP over the random BS cluster allocation increases with the cellular network density.

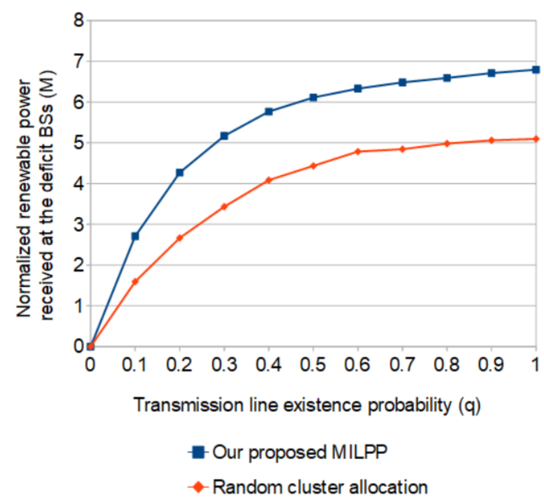

Fig. 6: Average normalized renewable power received at the deficit BSs (M) of our proposed MILPP and of random BS cluster allocation vs. transmission line existence probability (q).

Fig. 6 shows the performance of our proposed MILPP and of random BS cluster allocation for different transmission line existence probabilities (q). The performance gap between the two BS cluster allocations increases with the transmission line existence probability in the range of 0 to 0.3 whereas it is nearly constant in the range of 0.3 to 1.

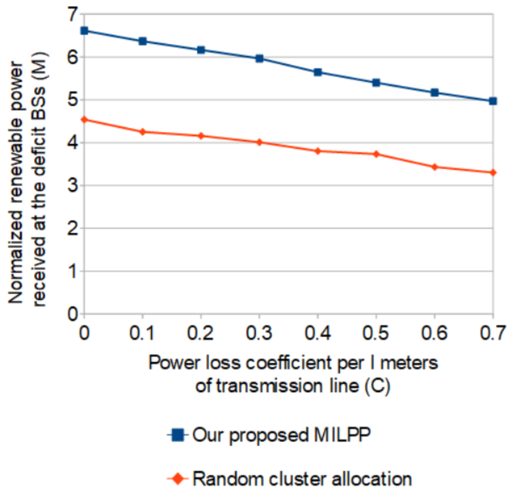

Fig. 7: Average normalized renewable power received at the deficit BSs (M) of our proposed MILPP and of random BS cluster allocation vs. power loss coefficient per l meters of transmission line (C).

Fig. 7 shows the performance of our proposed MILPP and of random BS cluster allocation for different power loss coefficients per l meters of transmission line (C). The performance gap between the two BS cluster allocations decreases slightly with the power loss coefficient per l meters of transmission line.

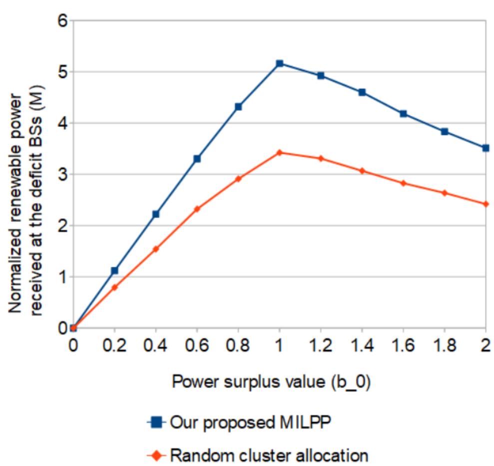

Fig. 8: Average normalized renewable power received at the deficit BSs (M) of our proposed MILPP and of random BS cluster allocation vs. power surplus value (b_0). b_1 was fixed to -1.

Fig. 8 shows the performance of our proposed MILPP and of random BS cluster allocation for different power surplus values (b_0). b_1 was fixed to -1. The performance gap between the two BS cluster allocations increases with the power surplus value in the range of 0 to 1 whereas it decreases in the range of 1 to 2. This is because the power was normalized with respect to $\max\{b_0, |b_1|\}$. If $b_0 \neq 1$, either $\hat{b}_0$ or $|\hat{b}_1|$ is smaller than 1 because a mismatch exists between the power surplus value and the power deficit value. Only if $b_0 = 1$, $\hat{b}_0$ and $|\hat{b}_1|$ are both 1 because the power surplus value and the power deficit value have the same absolute value.

Figs. 5 - 8 show that our proposed MILPP always outperforms the random BS cluster allocation because the MILPP considers the topology of the cellular network and the power losses in the transmission lines. Hence, our proposed MILPP will more likely deploy neighboring by transmission line connected base stations with different types of energy harvesters than the random BS cluster allocation.

V. Conclusion

We have developed a base station (BS) clustering optimization algorithm based on a mixed-integer linear programming problem (MILPP) that can be run once during the cellular network planning to determine for every BS which type of energy harvester should be optimally equipped to it, i.e., BSs grouped into one cluster by the algorithm are equipped with the same type of energy harvester. There are two different types of energy harvesters, which have anti-correlated energy generation profiles, available for deployment (two clusters). The optimization objective is to maximize the renewable power that can be shared in the cellular network. The MILPP takes into account the topology of the cellular network, i.e., whether or not a transmission line exists between a pair of BSs, and the distance-dependent power loss in the transmission lines during the optimization. We investigate the performance of our proposed MILPP in comparison with randomly allocating the BSs into clusters, i.e., without considering the topology of the cellular network or the power losses in the transmission lines. Hence, our proposed MILPP has a better performance because it will more likely deploy neighboring by transmission line connected base stations with different types of energy harvesters than the random BS cluster allocation. The normalized renewable power received at the BSs of our proposed MILPP in comparison with the random BS cluster allocation is on average around 40% higher.

Acknowledgment

This work was supported by the A*STAR-Sheffield Research Attachment Programme. This project has received funding from the European Unions Horizon 2020 research and innovation programme under the Marie Skłodowska-Curie grant agreement No 645705.

References

[1] X. Huang and N. Ansari, “Energy sharing within EH-enabled wireless communication networks,” *IEEE Wireless Communications*, vol. 22, no. 3, pp. 144–149, Jun 2015.

[2] Y. K. Chia, S. Sun, and R. Zhang, “Energy cooperation in cellular networks with renewable powered base stations,” *IEEE Transactions on Wireless Communications*, vol. 13, no. 12, pp. 6996–7010, Dec 2014.

[3] Y. Mao, Y. Luo, J. Zhang, and K. B. Letaief, “Energy harvesting small cell networks: feasibility, deployment, and operation,” *IEEE Communications Magazine*, vol. 53, no. 6, pp. 94–101, Jun 2015.

[4] D. Benda, S. Sun, X. Chu, T. Q. S. Quek, and A. Buckley, “PV cell angle optimization for energy generation-consumption matching in a solar powered cellular network,” *IEEE Transactions on Green Communications and Networking*, vol. 2, no. 1, pp. 40–48, Mar 2018.

[5] European Commission. (2016) Photovoltaic geographical information system (pvgis). [Online]. Available: http://re.jrc.ec.europa.eu/pvgis/

[6] H. Cole and D. Sang, *Revise AS Physics for AQA A*. Oxford, United Kingdom: Heinemann Educational Publishers, 2001, pp. 67–68.